Biochemical and Biophysical Research Communications 479 (2016) 496–501

Contents lists available at ScienceDirect

Biochemical and Biophysical Research Communications

journal homepage: www.elsevier.com/locate/ybbrc

Structural and functional analysis of the ASM p.Ala359Asp mutant that causes acid sphingomyelinase deficiency

Mariana Acuña [a, b, *, 1], Víctor Castro-Fernández [c, **, 1], Mauricio Latorre [b, d, e], Juan Castro [a], Edward H. Schuchman [f], Victoria Guixé [c], Mauricio González [b, d], Silvana Zanlungo [a, b, *]

[a] Departamento de Gastroenterología, Facultad de Medicina, Pontificia Universidad Católica de Chile, Santiago, Chile
[b] Center of Genome Regulation (Fondap 15090007), Universidad de Chile, Santiago, Chile
[c] Departamento de Biología, Facultad de Ciencias, Universidad de Chile, Santiago, Chile
[d] Laboratorio de Bioinformática y Expresión Génica, INTA, Universidad de Chile, Santiago, Chile
[e] Mathomics, Center for Mathematical Modeling, Universidad de Chile, Santiago, Chile
[f] Department of Genetics & Genomic Sciences, Icahn School of Medicine at Mount Sinai, New York, NY, USA

ARTICLE INFO

Article history:
Received 1 September 2016
Accepted 19 September 2016
Available online 20 September 2016

Keywords:
Niemann-pick disease
Acid sphingomylienase
SMPD1 mutations
p.Ala359Asp

ABSTRACT

Niemann-Pick disease (NPD) type A and B are recessive hereditary disorders caused by deficiency in acid sphingomyelinase (ASM). The p.Ala359Asp mutation has been described in several patients but its functional and structural effects in the protein are unknown. In order to characterize this mutation, we modeled the three-dimensional ASM structure using the recent available crystal of the mammalian ASM as a template. We found that the p.Ala359Asp mutation is localized in the hydrophobic core and far from the sphingomyelin binding site. However, energy function calculations using statistical potentials indicate that the mutation causes a decrease in ASM stability. Therefore, we investigated the functional effect of the p.Ala359Asp mutation in ASM expression, secretion, localization and activity in human fibroblasts. We found a 3.8% residual ASM activity compared to the wild-type enzyme, without changes in the other parameters evaluated. These results support the hypothesis that the p.Ala359Asp mutation causes structural alterations in the hydrophobic environment where ASM is located, decreasing its enzymatic activity. A similar effect was observed in other previously described NPDB mutations located outside the active site of the enzyme. This work shows the first full size ASM mutant model describe at date, providing a complete analysis of the structural and functional effects of the p.Ala359Asp mutation over the stability and activity of the enzyme.

1. Introduction

Niemann-Pick disease types A and B (NPDA and NPDB) are metabolic disorders in which harmful quantities of sphingomyelin are accumulated in the body organs. Both diseases are caused by pathogenic mutations in the *SMPD1* gene that encodes for the acid sphingomyelinase (ASM) enzyme. NPDA patients exhibit hepatosplenomegaly, progressive psychomotor deterioration and respiratory failure, and do not survive past early childhood. In contrast, NPDB is clinically heterogeneous and its onset is usually in mid-childhood. Most patients exhibit visceral involvement with little or no neurological involvement, allowing survival into adulthood [1,2]. NPD patients with intermediate phenotypes between types A and B have also been described, representing the expected continuum spectrum caused by the inheritance of different mutations in the *SMPD1* gene [3,4].

ASM is a lysosomal hydrolase responsible for sphingomyelin breakdown into phosphocholine and ceramide [5]. Within this organelle, ASM performs an essential function maintaining the dynamics of the membrane, causing reorganization of micro-

* Corresponding authors. Pontificia Universidad Católica de Chile, Departamento de Gastroenterología, Marcoleta 367, Santiago 8330024, Chile.
** Corresponding author. Universidad de Chile, Facultad de Ciencias, Departamento de Biología, Las Palmeras 3425, Santiago 7800003, Chile.
E-mail addresses: mariana.acuna1@gmail.com (M. Acuña), vcasfe@ug.uchile.cl (V. Castro-Fernández), silvana@med.puc.cl (S. Zanlungo).
[1] Contributed equally to this work.

http://dx.doi.org/10.1016/j.bbrc.2016.09.096
0006-291X/

domains and stimulating downstream signaling events [6]. In addition, ASM is the major responsible for ceramide levels in cells, an important signaling lipid involved in different cellular responses [7].

Currently, more than a hundred different mutations have been described for this enzyme [8–11]. In an attempt to understand how these mutations affect the function of the enzyme, different genotype/phenotype correlations have been done [8–10,12]. Recently, the crystallographic structure of the human ASM (hASM) (PDB: 5JG8) was published [13], where the SAP domain is shown in an open configuration. At the same time, different structures of ASM from mouse [14], highlighting the open (PDB: 5FIB) and closed (PDB: 5FI9) conformations of the SAP domain were reported, providing an excellent opportunity to establish correlations between the effect of the mutations described and its spatial position in the enzyme structure.

Recently, we studied the p.Ala359Asp (c.1076C > A) mutation of the ASM that causes NPDB in the Chilean population [12]. We described the clinical characteristics of 13 homozygous patients for this mutation, all of them showing a moderate to severe NPDB phenotype. Also, we established that the frequency of p.Ala359Asp in the healthy population is 1/105.7, which is higher than expected for the estimated number of NPDB patients reported. These results provided important information in terms of the clinical characterization and epidemiological incidence of p.Ala359Asp in the Chilean population.

In order to advance in the characterization of this ASM mutation and taking advantage of the current new information regarding the human sphingomyelinase structure, we generated a complete homology model of the p.Ala359Asp-ASM mutant. The structural analysis indicates that the mutation predominantly produces alterations in the surface of the protein in terms of the electrostatic potential and stability, with no alterations in the active site or in zinc ions coordination. To correlate these findings with the functional effect of this mutation, we characterized the expression and enzyme activity of p.Ala359Asp-ASM in human skin fibroblasts, al well as its lysosomal localization using a green fluorescent protein reporter. The results obtained indicate that p.Ala359Asp-ASM activity is significant lower than the wild-type protein. However, we did not find changes in the expression or destination of the protein. Considering published data [14] and our own results, the mutation is located outside the active site of the enzyme, similar to other previously described *SMPD1* mutations that cause NPDB. Finally, this work describes the first full size protein model of an ASM mutant described at date, providing a simple and effective *in silico* approach for the characterization of other ASM mutants.

2. Material and methods

2.1. Homology model in the closed conformation of hASM and p.Ala359Asp mutant

We modeled the p.Ala359Asp-ASM with the Modeller 9.15 software [15] using the closed conformation of ASM from *Mus musculus* (PDB: 5FI9) as template [14], and catalityc domain of the hASM (PDB: 5JG8) [13]. The open conformation of p.Ala359Asp was modeled only with 5JG8 as template. Fifty models were constructed, and from these, the best 10 potential DOPE models were chosen. Their quality was evaluated with PROSA2003 [16], Procheck [17] and VERIF3D [18] to choose the best model.

2.2. Macromolecular electrostatics calculation and prediction of the effect of mutations on protein stability

The Poisson-Boltzmann electrostatic potential surface was calculated with APBS [19] in Pymol [20], with protonation states corresponding to the lysosomal pH value of 5.0. The protonation state of the ionizable residues was calculated using PROPKA, atomic charges and radii were assigned from AMBER force field using PDB2PQR software [21]. The surface potentials were calculated at 0.15 M ionic concentration, 310 K, with a dielectric constant of 2.0 for protein and 78.0 for solvent. The effect of the mutation on protein stability was evaluated by function energy calculations using statistical potentials with DUET [22].

2.3. Cell culture

Human skin fibroblasts were maintained in DMEM supplemented with 10% (v/v) FBS and 1% (v/v) penicillin-streptomycin. The control and homozygous p.Ala359Asp NPDB skin fibroblasts were established from biopsies obtained at the Pontificia Universidad Católica de Chile after informed consent and with the approval of our Institutional Review Board.

2.4. Quantitative real-time reverse transcriptase-polymerase chain reaction assay

Total RNA was extracted from the fibroblast, pretreated with DNase I (Invitrogen, Carlsbad, CA, USA), and then reverse-transcribed to cDNA using random primers (Invitrogen). Real-time polymerase chain reactions (qPCR) were performed by SYBR Green I chemistry (SYBR Green PCR Master Mix, Applied Biosystems, Naerum, Denmark) with 25 ng of template cDNA and specific primers present at 200 μM using the ABI 7500 sequence detection system (Applied Biosystems). Primers sequences: *SMPD1*: CTCGGGCTGAAGAAGGAACCCA (F) and AGCGTCTCCACACCTCCACCAT (R). 18S: GTAACCCGTTGAACCCCATT (F) and CCATCCAATCGGTAGTAGCG (R).

2.5. Immunoblotting

Cell extracts (10 μg) were resolved by SDS-PAGE and transferred onto nitrocellulose membranes. Membranes were blocked by overnight incubation at 4 °C in 5% (w/v) milk powder dissolved in Tris-buffered saline (TBS) and 0.1% (w/v) Tween 20 (TBST). The membranes were then rinsed in TBST and incubated at room temperature for 2 h in the presence of a polyclonal anti-ASM antibody from Abcam (CAT #ab83354) (1:2000 dilution). The membranes were washed again in TBST, and incubated at room temperature for 2 h in the presence of a HRP conjugated anti-rabbit IgG antibody (1:5000 dilution).

2.6. In vitro acid sphingomyelinase assay

The ASM activity was measured using the “Acid sphingomyelinase activity kit” from Echelon Bioscience Incorporated (Salt Lake City, UT, USA). Briefly, the fibroblast samples were resuspended in 100 μL 1 mM PMSF/water and subjected to 3 freeze-thaw cycles. 20 μL of the samples and the diluted standards were loaded into the 96-well plate. 30 μL of the substrate buffer were added and 5 min later 50 μL of the diluted ASM substrate were added to each well. The plate was incubated at 37 °C for 3 h with shaking. Then, 50 μL of the stop buffer was added and after 10 min at room temperature the plate was read at 360 nm excitation and 460 nm emission. The values were calculated using the standard curve and normalized to protein concentration measured with the BCA kit (Thermo Scientific, Rockford, IL, USA).

2.7. ASM vectors and localization

The constructs carrying ASM fused to green fluorescent (ASM-GFP) were generated using the pcDNA3.1(−) plasmids containing the wild-type ASM [8] and the p.Ala359Asp mutation previously generated by us [12]. The complete cDNA of wild-type and p.Ala359Asp ASM were amplified using Pfx DNA polymerase (Invitrogen) and the following primers: 5′ GTAGGAAGCGCGACAATGCCCCGCTAC 3′ (sense) and 5′ GTGAAAGCTTGCAAAACAGTGGCCTTGGCCA 3′ (antisense). To generate the fusion protein the complete cDNA was cloned using the "CT-GFP fusion TOPO expression kit" (Invitrogen) according to the manufacturer's instructions. Both constructs were sequenced to ensure that the C-terminal GFP tag was in-frame with the ASM cDNA.

Transfections of these constructs were performed using the Lipofectamine 2000 reagent (Invitrogen) into HEK293T cells, according to the manufacturer's instructions. 47 h post-transfection the cells were treated with Lysotracker-Red probe (Invitrogen). The medium was removed and the prewarmed (37 °C) 500 nM probe-containing medium was added and incubated for 1 h. The cells were then washed, fixed and mounted with fluoromount. Fluorescent images were captured with a confocal Olympus microscope (Olympus, Tokyo, Japan).

2.8. Nomenclature

Two nomenclatures have been used for describing the mutations in NPDA/B: the "historical" nomenclature that refers to a reference sequence that lacks two codons due to a naturally occurring length polymorphism in the signal peptide portion of the *SMPD1* gene, and the "current" nomenclature which includes these two codons. In this paper the p.Ala359Asp (c.1076C > A) mutation was named and the three-dimensional model was generated using the current gene sequence (RefSeq NM_000543.3). In some cases we included the historical nomenclature to facilitate reading for clinicians and investigators with a general knowledge of NPDA/B.

3. Results and discussion

3.1. Model of the sphingomyelinase p.Ala359Asp mutant

The structure of the hASM has three regions. The SAP domain consists of four α-helices stabilized by three disulphide bonds, a connector region of 167–198 residues rich in prolines, and a catalytic domain that belongs to the calcineurin-like phosphoesterase family (PFAM code: PF00149) consisting in two 6-stranded β-sheets surrounded by a ring of α-helices [13]. As expected, the homology model of the p.Ala359Asp-ASM model agrees with the crystal structure of the human sphingomyelinase, where the orientation and positioning of the three distinct regions present in the wild-type ASM (SAP, connector and catalytic domain) are not affected by the mutation (Fig. 1A). The crystallographic structure of hASM only describes the open conformation of the SAP domain. Considering this, in order to study the effect of the mutation in the two possible conformations we modeled the closed conformation of the hASM for the wild-type and p.Ala359Asp mutant. We used the closed conformation describe in the mouse protein (PDB: 5FI9) as template and the catalytic model of the hASM (PDB: 5JG8, residues 174 to 611) (Fig. 1B).

In the open conformation, the distance from the p.Ala359Asp position to the SAP domain (center of mass) and to the Zn^{2+} ions of the active site were 45 Å and 20–21 Å respectively. In the closed conformation the mutation was located 38 Å from the SAP domain (center of mass) and 22–23 Å from Zn^{2+} ions of the active site. In both conformations (open and closed) the distance between the p.Ala359Asp mutation and either the SAP or the catalytic domain are far enough to suggest that the residue does not participate directly in lipid binding (SAP) or in sphingomyelin breakdown (catalytic). Previous reports indicate that the Ala359 residue is part of or is located near the substrate-binding region [23,24]. However, our results demonstrated that this residue is located in an α-helix far from the active site, with its lateral chain pointing to the hydrophobic core of the protein and surrounded by the lateral chains of the hydrophobic residues Leu355, Pro356, Leu363, Tyr369 and Leu371. Residue Ala359 is buried into the protein with a relative accessibility to the solvent of only 0.1% Therefore, the change of this residue to Asp would elicit a dramatic disturbance in this hydrophobic environment.

To estimate local changes in stability between the wild-type and the p.Ala359Asp-ASM enzymes, we performed function energy calculations using statistical potentials (Fig. 1C). The results indicate that, in terms of the pseudo energy parameter (ΔΔG), the mutation causes a protein destabilization of −3.65 kcal/mol (Site Directed Mutator, SDM) [25] and of −2.57 kcal/mol according to the DUET web server [22]. Considering that protein overall stability is usually between 5 and 10 kcal/mol, the ΔΔG change caused by p.Ala359Asp strongly suggest a destabilization of the hydrophobic core. As was described before, most of the

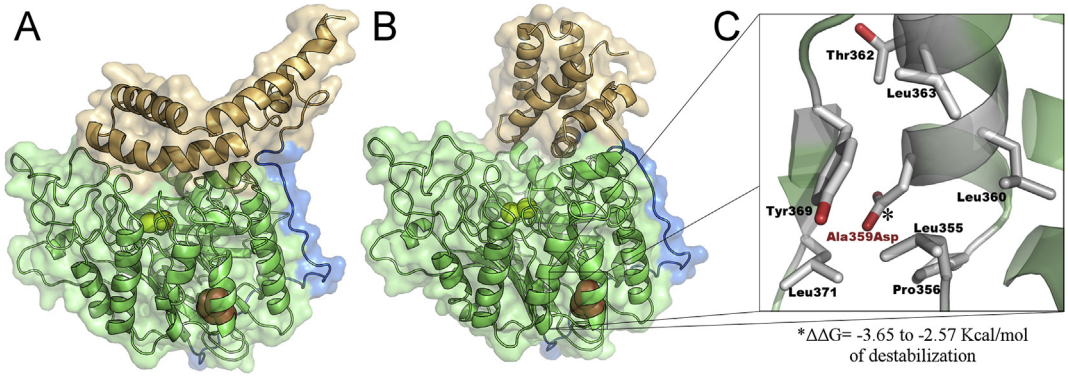

Fig. 1. Homology model of p.Ala359Asp-ASM. A) open conformation, B) closed conformation, C) local hydrophobic environment of p.Ala359Asp. Our model includes aminoacids 85 to 613. The SAP domain is colored in light brown (residues 85 to 170), the catalytic domain in green (residues 200 to 613) and the rich proline linker in blue (residues 171 to 199). p.Ala359Asp is indicated as red spheres. Zinc ions are shown as yellow spheres. (For interpretation of the references to colour in this figure legend, the reader is referred to the web version of this article.)

already characterized mutations potentially responsible for disease, destabilize the folded state by about 2–3 kcal/mol, suggesting that mutations that in fact cause the pathology would be in this range [26].

Next, we evaluated changes in the electrostatic surface potential in the open and closed conformations caused by the p.Ala359Asp using Poisson-Boltzmann (Fig. 2). In the wild-type ASM structures we observed several changes in the electrostatic surface potential between the closed and the open conformation. In particular, we found great differences at the active site. The open conformation presented an extremely negative surface around the SM binding site, whereas the closed conformation presented a neutral distribution, with a negative zone limited to the Zn^{2+} ions binding site. The rest of the ASM surface mainly shows a positive distribution at pH 5.0 in both conformations. Interestingly, the positive charge of the surface has been described as necessary for the interaction with the negative charges of the lysosome membrane [27]. On the other hand, the predominantly negative charge observed at the active site in the open conformation described here may be a mechanism for discrimination of positively charged lipids, favoring the interaction with the positive choline group of the sphingomyelin.

While the mutation does not affect the electrostatic potential of the active site, its presence clearly induces a local change over the protein surface in both conformations, mainly in the open one, changing from a neutral charged zone in the wild-type ASM to a charged zone in p.Ala359Asp ASM. Interestingly, similar perturbations in protein stability consistent with a set of structural effects, such as reduction in hydrophobic area and loss of electrostatic interactions among others, have been observed in different human proteins affected by single residue mutations [26]. All these data strongly support the idea that the p.Ala359Asp mutation causes a general destabilization of the protein structure including the active site of the ASM, which probably explains the protein malfunction in NPDB disease by acting as a long range effect mutation.

According to the recently published structure, 103 mutations were located in the catalytic core, 19 in the C-terminal subdomain, 8 in the saposin domain and 4 in the Pro-rich linker, and most of them are predicted to affect the fold or stability of ASM [14]. Our analysis of some of the published mutations suggests that most of those that cause NPDA disease are located closely to the active site, producing alterations in the activity of the enzyme or in the coordination of Zn^{2+} ions (Supplementary Table I). On the other hand, NPDB mutations are mainly located on the protein surface, modifying the ionic charges of amino acids and therefore causing changes in protein structure stability. This differential localization of mutations could explain in part the degrees of severity observed in both NPD types.

3.2. *ASM expression and enzymatic activity in wild-type and p.Ala359Asp fibroblasts*

To determine the consequences of the p.Ala359Asp mutation in protein function we cultured skin fibroblasts from a control individual and from a patient homozygous for this mutation, under standard conditions. First, we evaluated the transcript and protein expression of the enzyme and we found no differences between the control and the patient's cells (Fig. 3A and B). Also, we did not find differences in the protein levels of the culture media, corroborating that the secretion of the mutant protein is similar to the secretion of the control ASM (Fig. 3C). To evaluate if the p.Ala359Asp mutation interferes with the correct destination of the ASM to lysosomes we generated the fusion proteins wild-type-ASM-GFP and p.Ala359Asp-ASM-GFP. We corroborated that both proteins are sorted to the lysosome, since the GFP reporter co-localizes with the lysotracker marker (Fig. 3E).

Finally, we measured ASM activity *in vitro* and found a significant difference between the enzyme from wild-type and p.Ala359Asp fibroblasts being the activity of the mutant protein 3.8% of the wild-type activity (Fig. 3D). This findings are

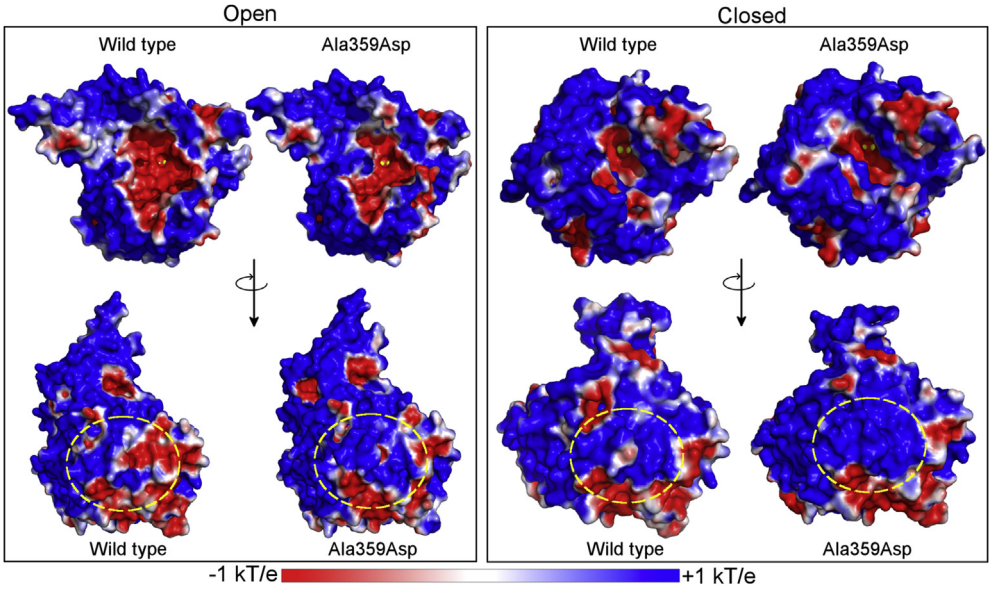

Fig. 2. Electrostatic potential changes induced by the p.Ala359Asp. Active site view (upper models) and p.Ala359Asp localization (lower models, dashed line circle). Zn^{2+} ions are shown as yellow spheres in the active site. Poisson-Boltzmann electrostatic potential was calculated at pH 5, 0.15 M of ions concentration and colored by potential solvent accessible surface. (For interpretation of the references to colour in this figure legend, the reader is referred to the web version of this article.)

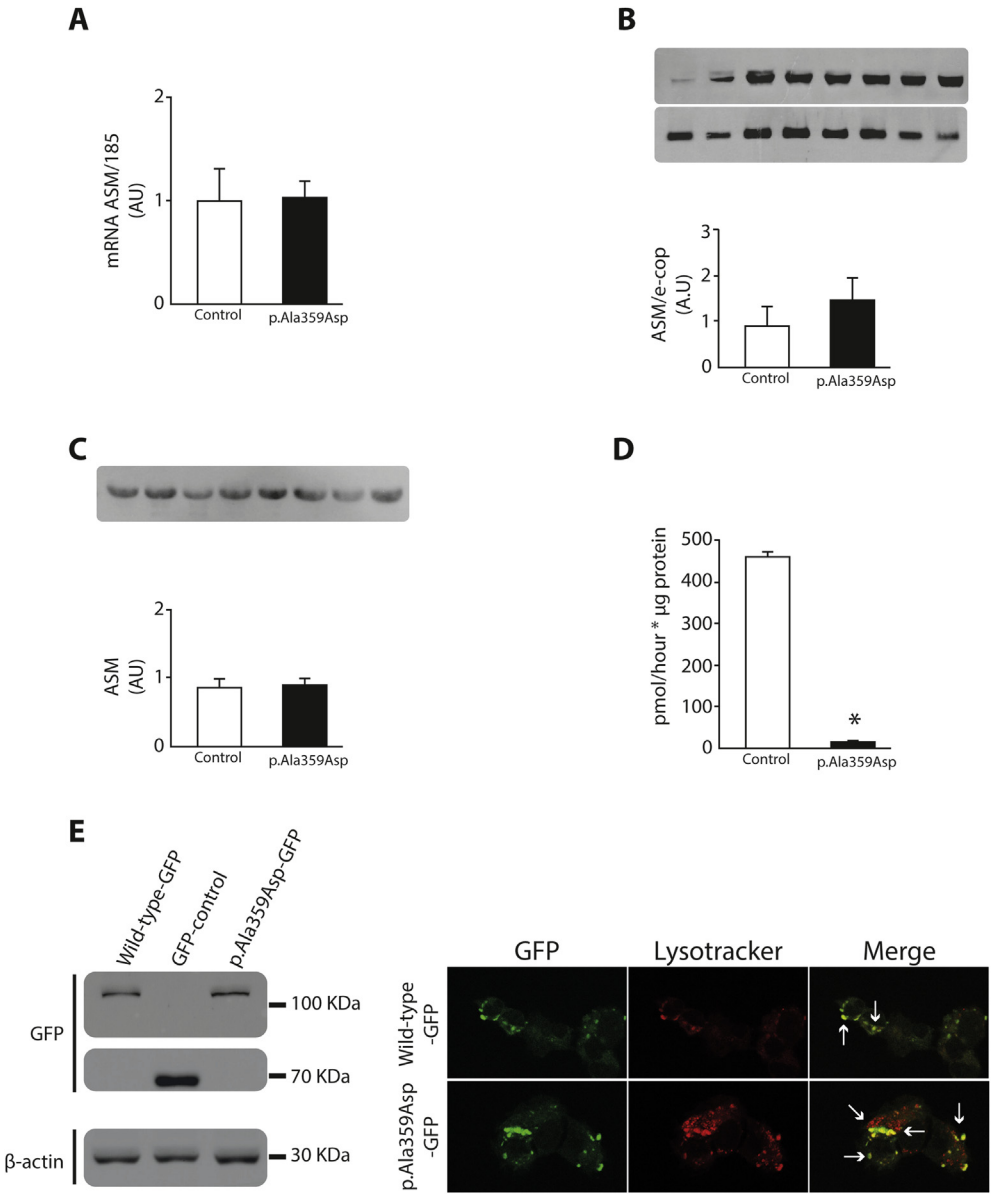

Fig. 3. Homozygous p.Ala359Asp-ASM abundance, sorting and enzymatic characterization. Analysis of ASM: A) mRNA relative expression, B) protein expression, C) Protein levels in the culture media D) ASM activity, in control fibroblasts and in p.Ala359Asp mutant patient fibroblasts. E) Analysis of HEK293T cells transfected with wild-type-ASM-GFP and p.Ala359Asp-ASM-GFP fusion proteins. Protein levels and localization of the constructs. Fluorescence microscopy shows Lysotracker-red (lysosomal marker) and GFP fusion proteins. Colocalization is seen as yellow color (arrows), as the result of the merging of the GFP reporter with the Lysotracker-red. (For interpretation of the references to colour in this figure legend, the reader is referred to the web version of this article.)

consistent with the site-directed mutagenesis and transient transfection assays in COS-7 cells we reported before, showing that the p.Ala359Asp mutation significantly reduces ASM activity to 4.2% of the wild-type enzyme without affecting protein levels [12]. This residual activity is similar to that observed in other NPDB mutants [8,11,28–30]. In addition, as it has been described for other variants, the fact that NPD patients have normal expression levels of the ASM protein predicts that the frequency and/or severity of immunologically related infusion reactions to enzyme replacement therapy (ERT) could be less severe than in other diseases where deletion mutations are common [24]. Moreover, the fact that the ASM protein is expressed at normal levels opens the possibility of using small molecules to enhance the activity of the enzyme.

Competing interests

Edward H. Schuchman is an inventor on several patents licensed to Genzyme, a Sanofi Corporation, which describes the diagnosis and treatment of NPD. Silvana Zanlungo has received research grants from Genzyme, a Sanofi Corporation. Mariana Acuña, Víctor Castro-Fernández, Mauricio Latorre, Victoria Guixé and Mauricio González declare that they have no conflict of interest.

Acknowledgement

This work was supported by grants from the Fondo Nacional de Desarrollo Científico y Tecnológico (FONDECYT) [grant number 1150816] to S.Z, [grant number 1150460] to V.G; [grant number

11150679] to M.L; Fondo Nacional de Desarrollo de Areas Prioritarias, FONDAP Center for Genome Regulation (CGR) [Project number 15090007] to S.Z, M.G and M.L.; Genzyme grant "Assessment of the A359D acid sphingomyelinase gene mutation frequency in the Chilean population" to E.H.S and S.Z; Comisión Nacional de Ciencia y Tecnología (CONICYT) PhD student grant [number 21120490] to M.A and FONDECYT Postdoctorado [grant number 3160332] to V.C-F; National Institutes of Health grant HD28607 to E.H.S.

Appendix A. Supplementary data

Supplementary data related to this article can be found at http://dx.doi.org/10.1016/j.bbrc.2016.09.096.

References

[1] E.H. Schuchman, The pathogenesis and treatment of acid sphingomyelinase-deficient Niemann-Pick disease, J. Inherit. Metab. Dis. 30 (2007) 654–663.
[2] M.P. Wasserstein, R.J. Desnick, E.H. Schuchman, S. Hossain, S. Wallenstein, C. Lamm, et al., The natural history of type B Niemann-Pick disease: results from a 10-year longitudinal study, Pediatrics 114 (2004) e672–677.
[3] M.P. Wasserstein, A. Aron, S.E. Brodie, C. Simonaro, R.J. Desnick, M.M. McGovern, Acid sphingomyelinase deficiency: prevalence and characterization of an intermediate phenotype of Niemann-Pick disease, J. Pediatr. 149 (2006) 554–559.
[4] H. Pavlu-Pereira, B. Asfaw, H. Poupctova, J. Ledvinova, J. Sikora, M.T. Vanier, et al., Acid sphingomyelinase deficiency. Phenotype variability with prevalence of intermediate phenotype in a series of twenty-five Czech and Slovak patients. A multi-approach study, J. Inherit. Metab. Dis. 28 (2005) 203–227.
[5] R.O. Brady, J.N. Kanfer, M.B. Mock, D.S. Fredrickson, The metabolism of sphingomyelin. II. Evidence of an enzymatic deficiency in Niemann-Pick disease, Proc. Natl. Acad. Sci. U. S. A. 55 (1966) 366–369.
[6] S. Falcone, C. Perrotta, C. De Palma, A. Pisconti, C. Sciorati, A. Capobianco, et al., Activation of acid sphingomyelinase and its inhibition by the nitric oxide/cyclic guanosine 3',5'-monophosphate pathway: key events in Escherichia coli-elicited apoptosis of dendritic cells, J. Immunol. 173 (2004) 4452–4463.
[7] L. Arana, P. Gangoiti, A. Ouro, M. Trueba, A. Gomez-Munoz, Ceramide and ceramide 1-phosphate in health and disease, Lipids Health Dis. 9 (2010) 15.
[8] J.P. Desnick, J. Kim, X. He, M.P. Wasserstein, C.M. Simonaro, E.H. Schuchman, Identification and characterization of eight novel SMPD1 mutations causing types A and B Niemann-Pick disease, Mol. Med. 16 (2010) 316–321.
[9] C.M. Simonaro, R.J. Desnick, M.M. McGovern, M.P. Wasserstein, E.H. Schuchman, The demographics and distribution of type B Niemann-Pick disease: novel mutations lead to new genotype/phenotype correlations, Am. J. Hum. Genet. 71 (2002) 1413–1419.
[10] S. Zampieri, M. Filocamo, A. Pianta, S. Lualdi, L. Gort, M.J. Coll, et al., SMPD1 mutation update: database and comprehensive analysis of published and novel variants, Hum. Mutat. 37 (2) (2016) 139–147.
[11] T. Takahashi, M. Suchi, R.J. Desnick, G. Takada, E.H. Schuchman, Identification and expression of five mutations in the human acid sphingomyelinase gene causing types A and B Niemann-Pick disease. Molecular evidence for genetic heterogeneity in the neuronopathic and non-neuronopathic forms, J. Biol. Chem. 267 (1992) 12552–12558.
[12] M. Acuna, P. Martinez, C. Moraga, X. He, M. Moraga, B. Hunter, et al., Epidemiological, clinical and biochemical characterization of the p. (Ala359Asp) SMPD1 variant causing Niemann-Pick disease type B, Eur. J. Hum. Genet. 24 (2) (2016) 208–213.
[13] Z.J. Xiong, J. Huang, G. Poda, R. Pomes, G.G. Prive, Structure of human acid sphingomyelinase reveals the role of the saposin domain in activating substrate hydrolysis, J. Mol. Biol. 438 (5) (2016) 3026–3042.
[14] A. Gorelik, K. Illes, L.X. Heinz, G. Superti-Furga, B. Nagar, Crystal structure of mammalian acid sphingomyelinase, Nat. Commun. 7 (2016) 12196.
[15] N. Eswar, B. Webb, M.A. Marti-Renom, M.S. Madhusudhan, D. Eramian, M.Y. Shen, et al., Comparative protein structure modeling using MODELLER, Curr. Protoc. Protein Sci. (2007). Book chaper 2.9, pages: 2.9.1–2.9.31.
[16] M. Wiederstein, M.J. Sippl, ProSA-web: interactive web service for the recognition of errors in three-dimensional structures of proteins, Nucleic Acids Res. 35 (2007) W407–W410.
[17] R.A. Laskowski, M.W. Macarthur, D.S. Moss, J.M. Thornton, Procheck - a program to check the stereochemical quality of protein structures, J. Appl. Crystallogr. 26 (1993) 283–291.
[18] R. Luthy, J.U. Bowie, D. Eisenberg, Assessment of protein models with three-dimensional profiles, Nature 356 (1992) 83–85.
[19] N.A. Baker, D. Sept, S. Joseph, M.J. Holst, J.A. McCammon, Electrostatics of nanosystems: application to microtubules and the ribosome, Proc. Natl. Acad. Sci. U. S. A. 98 (2001) 10037–10041.
[20] L.L.C. Schrodinger, The PyMOL Molecular Graphics System, Version 1.8, 2015.
[21] T.J. Dolinsky, J.E. Nielsen, J.A. McCammon, N.A. Baker, PDB2PQR: an automated pipeline for the setup of Poisson-Boltzmann electrostatics calculations, Nucleic Acids Res. 32 (2004) W665–W667.
[22] D.E. Pires, D.B. Ascher, T.L. Blundell, DUET: a server for predicting effects of mutations on protein stability using an integrated computational approach, Nucleic Acids Res. 42 (2014) W314–W319.
[23] M. Seto, M. Whitlow, M.A. McCarrick, S. Srinivasan, Y. Zhu, R. Pagila, et al., A model of the acid sphingomyelinase phosphoesterase domain based on its remote structural homolog purple acid phosphatase, Protein Sci. 13 (2004) 3172–3186.
[24] I. Jones, X. He, F. Katouzian, P.I. Darroch, E.H. Schuchman, Characterization of common SMPD1 mutations causing types A and B Niemann-Pick disease and generation of mutation-specific mouse models, Mol. Genet. Metab. 95 (2008) 152–162.
[25] C.L. Worth, R. Preissner, T.L. Blundell, SDM–a server for predicting effects of mutations on protein stability and malfunction, Nucleic Acids Res. 39 (2011) W215–W222.
[26] P. Yue, Z. Li, J. Moult, Loss of protein structure stability as a major causative factor in monogenic disease, J. Mol. Biol. 353 (2005) 459–473.
[27] V.O. Oninla, B. Breiden, J.O. Babalola, K. Sandhoff, Acid sphingomyelinase activity is regulated by membrane lipids and facilitates cholesterol transfer by NPC2, J. Lipid Res. 55 (2014) 2606–2619.
[28] K. Ferlinz, R. Hurwitz, M. Weiler, K. Suzuki, K. Sandhoff, M.T. Vanier, Molecular analysis of the acid sphingomyelinase deficiency in a family with an intermediate form of Niemann-Pick disease, Am. J. Hum. Genet. 56 (1995) 1343–1349.
[29] W. Sperl, G. Bart, M.T. Vanier, H. Christomanou, I. Baldissera, E. Steichen-Gersdorf, et al., A family with visceral course of Niemann-Pick disease, macular halo syndrome and low sphingomyelin degradation rate, J. Inherit. Metab. Dis. 17 (1994) 93–103.
[30] V. Mihaylova, J. Hantke, I. Sinigerska, S. Cherninkova, M. Raicheva, S. Bouwer, et al., Highly variable neural involvement in sphingomyelinase-deficient Niemann-Pick disease caused by an ancestral Gypsy mutation, Brain 130 (2007) 1050–1061.